Terahertz Sources and Detectors Using Two-Dimensional Electronic Fluid in High Electron-Mobility Transistors

Michael S. Shur, *Fellow, IEEE,* and Jian-Qiang (James) Lü, *Member, IEEE*

***Abstract*—In this paper, we discuss our recent theoretical and experimental results dealing with plasma waves in high electron-mobility transistors (HEMT's) and their applications for sources and detectors operating in millimeter and submillimeter range. Plasma waves in short-channel HEMT's have a resonant response. The HEMT-based source or detector utilizing plasma waves should operate at much higher frequencies than conventional transit-time limited devices since the plasma waves propagate much faster than electrons.**

***Index Terms*—High electron-mobility transistor, plasma-wave electronics, terahertz detector, terahertz radiation.**

I. Introduction

The development of VLSI technology has led to a dramatic reduction in device sizes (from 10 μm or so in the 1960's to sub-0.1-μm in short silicon MOSFET's in the late 1990's). The critical device dimensions are becoming comparable to or even smaller than a mean free pass for electron collisions with impurities or phonons. At the same time, this reduction of device feature sizes results in a greatly increased electron density in the device channel [1], [2] since the gate voltage swing does not scale proportionally to the gate length and to the thickness of the gate oxide. As a consequence, electron–electron collisions become dominant, and electrons in an FET channel should behave as a two-dimensional (2-D) electron fluid, i.e., they should be governed by hydrodynamic equations [3], [4]. As was shown in [3] and [4], these equations coincide with those describing a water flow in shallow channels. The electron fluid in an FET channel can support surface plasma waves, similar to shallow water waves and to sound waves. The velocity of the plasma waves depends on the gate voltage swing and exceeds the electron drift velocity by an order of magnitude or so [3].

This result has profound consequences for the device behavior. First, a predicted instability of these plasma waves should result in the emission of terahertz radiation [3]. Some kind of terahertz emission from a GaAs-based high electron-mobility transistor (HEMT) in the right frequency range has been recently observed, even though the exact mechanism of such emission remains unclear [5]. Second, an FET should operate as a detector of microwave and submillimeter wave (i.e., terahertz) radiation [4]. Such detection has been observed at microwave frequencies for GaAs- and GaN-based HEMT's [6], [7] and at terahertz frequencies for GaAs-based HEMT's [8]. These results are encouraging for the new emerging field of plasma-wave electronics that has the promise of realizing sensitive terahertz detectors and discrete and array ("electronic flute" [9]) sources. However, many theoretical and experimental problems have to be resolved in order to justify these expectations. The problems, which should be addressed, include the role of the boundary conditions (i.e., to the role of contacts and external circuit [10]), the role of the viscosity of the electronic fluid [3], the transient response [11], the role of the plasma waves propagating under a certain angle to the gate [12], the mechanism of coupling of plasma waves with the electromagnetic radiation, the reflections of plasma waves from contact pads, the effect of the velocity saturation and of the plasma wave choking [13], and the role of the nonuniformities of the gate length along the channel [14].

In this paper, we review the theoretical predictions for plasma-wave electronics devices and recent experimental results for plasma-wave detectors of terahertz radiation.

II. Plasma-Wave Instability

Plasma waves in an FET have a linear dispersion law similar to sound waves, and an FET channel acts as a resonance cavity for plasma waves [3], [4]. A quality factor of such a cavity is on the order of $Q = s\tau/L$, where $s = (eU/\mathbf{m})^{1/2}$ is the velocity of the plasma waves, $\tau = \mu\mathbf{m}/e$ is the momentum relaxation time, and L is the channel length. Here, $\mathbf{m}$ is the electron effective mass, μ is a low field mobility, and U is the gate-bias swing. As was shown in [3], in a high-mobility short-channel FET, plasma-wave instability may occur due to the plasma-wave amplification (caused by the wave reflections from the channel boundaries).

Let us first assume that the gate voltage swing is fixed at U and the channel current is zero. The plasma-wave dispersion law $k = \pm\omega/s$ corresponding to the well-known shallow water waves is readily obtained from the linearized equation of motion and continuity equation [15], [16]. Here, ω is the frequency, k is the wave vector, and s is the wave velocity.

If the electrons move with a velocity v_o, the dispersion relation becomes $k = \omega/(v_o \pm s)$, which means that the waves are carried along by the flow.

Manuscript received March 18, 1999. This work was supported by the Office of Naval Research, Project Monitor, Dr. J. Zolper, and by the Army Research Office, Project Monitor, Dr. D. Woolard.

The authors are with the Department of Electrical Computer and Systems Engineering, Center for Integrated Electronics and Electronics Manufacturing, Rensselaer Polytechnic Institute, Troy, NY 12180-3590 USA.

Publisher Item Identifier S 0018-9480(00)02536-9.

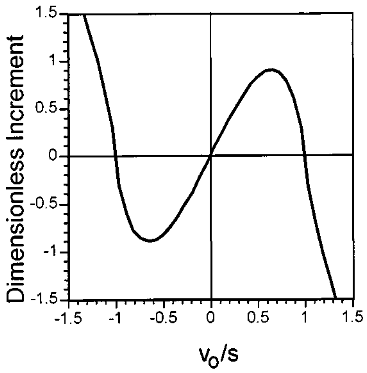

Fig. 1. Dimensionless plasma wave increment $2\omega'' L/s$ as a function of Mach number $M = v_o/s$. The steady electron flow is unstable when $0 < v_o < s$ and $v_o < -s$ [3].

We now consider the situation when the source and drain are connected to a current source and the gate and source are connected to a voltage source V_{GS}. The ac variation of the electric current at the source side of the channel is possible even for a constant external current since the ac current at the source is short circuited to the gate by the dc voltage source. These boundary conditions correspond to zero impedance at the source. A study of the temporal behavior of a small fluctuation superimposed on steady uniform flow leads to the following expressions for the real and imaginary parts $\omega = \omega' + i\omega''$:

$$\omega' = \frac{|s^2 - v_o^2|}{2Ls}\pi n \tag{1}$$

$$\omega'' = \frac{s^2 - v_o^2}{2Ls}\ln\left|\frac{s + v_o}{s - v_o}\right| \tag{2}$$

where n is an odd integer for $|v_o| < s$ and an even integer for $|v_o| > s$. Equation (2) (see also Fig. 1) shows that for $s > v_o > 0$, the steady electron flow is unstable at low electron velocities. The reason for the instability becomes clear if we consider wave reflections from each boundary.

The solution of linearized continuity equation and equation of motion shows that the reflection does not change the wave amplitude at $x = 0$ (where the voltage is fixed), while at $x = L$ (where the current is fixed), the amplitude ratio of the reflected and oncoming waves is $(s + v_o)/(s - v_o)$. Hence, the reflection from the boundary with the fixed current results in the wave amplification for $v_o < s$. Let $\tau = L/(s + v_o) + L/(s - v_o)$ be the time during which the wave travels from the source to the drain and back. During time t, the wave amplitude grows in $[(s + v_o)/(s - v_o)]^{t/\tau}$ times since t/τ is the number of wave round passages during time t. Equating $[(s + v_o)/(s - v_o)]^{t/\tau}$ to $\exp(\omega'' t)$, we obtain (2). Thus, the proposed new mechanism of plasma-wave generation is based on the amplification of the wave during its reflection from the device boundaries.

There are two decay mechanisms that oppose wave growth: external friction related to electron scattering by phonons or impurities, and internal friction caused by the viscosity of the electron fluid. The external friction leads to the addition of the $-1/(2/\tau)$ term to the wave increment. Hence, the wave grows only if the number of scattering events during the transit time is small. The viscosity v of the electron fluid causes an additional damping with the decrement of vk^2. Hence, the viscosity is especially effective in damping higher order modes. Comparing ω'' with vk^2 for the first mode, we find that the effect of the viscosity for $v_o = s$ is small when the Reynolds number $\text{Re} = Lv_o/v$ is much greater than unity. A very crude estimate yields $v \sim 15$ cm^2/s and $\text{Re} = mv_oL/\hbar \sim 12$ for $v_o = 10^7$ cm/s and $L = 0.2$ μm.

For a sample with $L = 0.2$ μm at 77 K ($\tau \sim 10^{-11}$ s), the increment v_o/L exceeds the decrement $1/(2\tau)$ caused by the collisions when $v_o > 10^6$ cm/s. For the same sample, the decrement caused by viscosity, i.e., $v(2\pi/L)^2/16$, is smaller than the increment v_o/L when $v_o > \pi^2 v/(4L) \sim 1.8 \times 10^6$ cm/s. Hence, the threshold velocity for the instability is well below the peak velocity in GaAs.

Once the electron velocity exceeds the threshold, the plasma waves grow. This growth should lead to oscillations for which the plasma-wave amplitude is limited by nonlinearity. The amplitude of these nonlinear oscillations should be comparable to gate-bias swing if the flow velocity is substantially larger than the threshold value.

The plasma oscillations result in a periodic variation of the channel charge and the mirror image charge in the gate contact, i.e., to the periodic variation of the dipole moment. This variation should lead to electromagnetic radiation. The device length is much smaller than the wavelength of the electromagnetic radiation λ_R at the plasma-wave frequency. Hence, the ballistic FET should operate as a point or linear source of electromagnetic radiation. Many such devices can be placed into a quasi-optical array for power combining [9]. The maximum radiation intensity is limited by the gate voltage swing. The maximum modulation frequency is still limited by the transit time (-2 ps in our example).

With an exception of a nonresonant FET detector described below, FET's utilizing plasma waves must be short enough so that parameter $Q = s\tau/L$ is greater than unity. This corresponds to the condition that can be written as [13]

$$L \ll L_{\text{cr}} = \frac{s\mu\mathbf{m}}{e}. \tag{3}$$

Criterion (3) coincides (within a numerical factor) with the requirement $\omega_o\tau \gg 1$. Also, for plasma-wave electronics (again, with an exception of the nonresonant FET detectors mentioned above), the frequency of operation has to be much higher than $\omega_{\text{cr}} = 1/\tau$. Fig. 2 shows the plots of L_{cr} versus gate bias for different material systems [13]. As can be seen from Fig. 2, the required dimensions are well within the range of typical dimensions for deep submicrometer FET's.

The region of instability on the *I–V* plot is represented in Fig. 3 [17]. The current–voltage characteristics in units $j_0 = C\mathbf{m}(L/\tau)^3/e$, $U_0 = \mathbf{m}(L/\tau)^2/e$ are plotted for different values of the parameter $\gamma = L/(s_s\tau)$. Here, C and s_s are the gate capacitance per unit area and the plasma-wave velocity at the source, respectively. The heavy line indicates the instability threshold. The dotted line corresponds to the choking threshold [18]. The two curves, which merge at point A, confine the instability region. Dashed lines indicate the unstable parts of the current–voltage characteristics. For $\gamma > 0.54$, the current–voltage characteristics are stable.

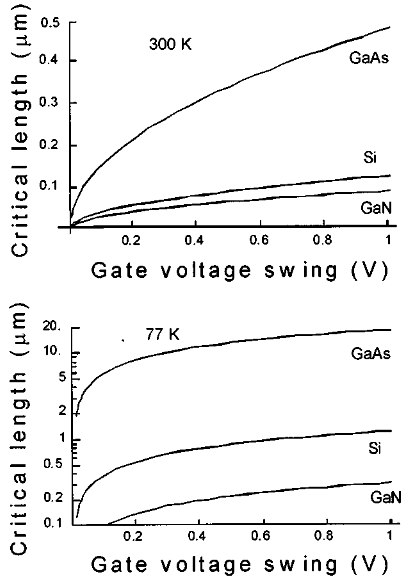

Fig. 2. L_{cr} versus gate bias for different material systems [13].

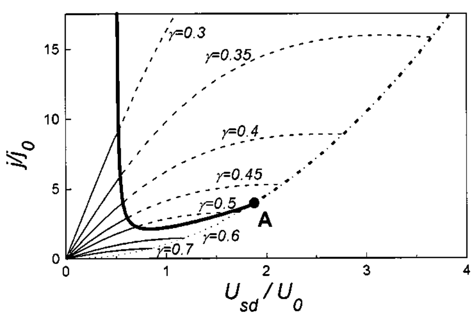

Fig. 3. The region of instability on the *I-V* plot for different values of the parameter γ. The heavy line indicates the instability threshold. The dotted line corresponds to the choking threshold. Dashed lines indicate the unstable parts of the *I-V* characteristics [17].

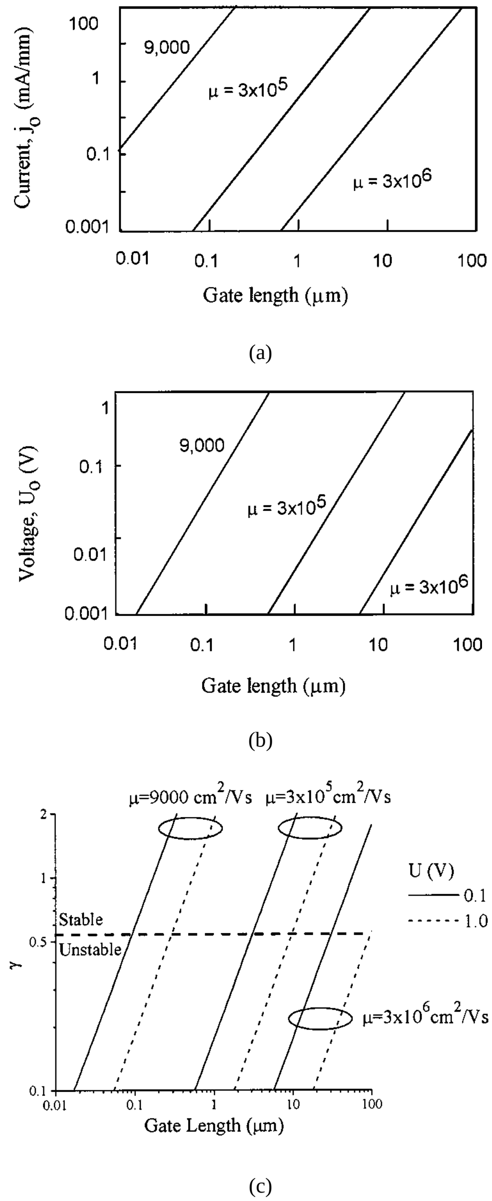

Fig. 4. Length dependence of parameters j_o, U_0, and γ [see (a)–(c)] for GaAs for different values of mobility (in cm^2/V·s). Numbers near the lines are the values of the low field mobility. The heavy dashed line in (c) represents the critical value of $\gamma = 0.54$ [17]. Parameters used in the calculation: electron effective mass: $\mathbf{m} = 0.063\mathbf{m}_0$, dielectric permittivity: $\varepsilon = 1.14 \times 10^{-10}$ F/m, gate-to-channel separation: $d = 10^{-8}$ m, gate voltage swing: $U = 0.1$ V for all solid lines, and $U = 1.0$ V for dashed line in (c).

Parameters j_o, U_0, and γ determine the scale of currents, voltages, and device parameters, which correspond to the instability region. Fig. 4 shows the length dependence of these three parameters for GaAs for different values of the 2-D electron mobility [17]. We chose the mobility values of 9000 cm^2/V·s, 300 000 cm^2/V·s, and 3 000 000 cm^2/V-·, which can be achieved in a 2-D electron gas (2DEG) in GaAs at 300, 77, and 4–20 K, respectively. As can be seen from Fig. 4, sub-0.1 micrometer dimensions, submicrometer dimensions, and dimensions on the order of several micrometers are required in order to observe the instability in the samples with the lowest, intermediate, and highest values of the electron mobility.

There are many unresolved problems that have to be addressed in order to observe this new instability. The role of electron fluid viscosity, and the role of boundary conditions and coupling between electromagnetic radiation and the plasma waves have to be better understood, and integrated antenna structures have to be designed. It is possible that effective coupling will be easier to achieve in periodic structures, such as proposed for an "electronic flute" [9].

III. Plasma-Wave Detectors

A short-channel FET should have a resonance response to electromagnetic radiation at the plasma oscillation frequency. A long-channel FET has a nonresonant response to electromagnetic radiation, and such an FET can be used as a broad-band detector for frequencies up to several tens of terahertz. Our estimates show that the sensitivity of the short-channel resonant FET detector should exceed the sensitivity of conventional Schottky diode detectors by a factor of Q^2. For a high mobility device, this factor could be several orders of magnitude. The sensitivity of the nonresonant broad-band HEMT detector is comparable to the sensitivity of conventional Schottky diode

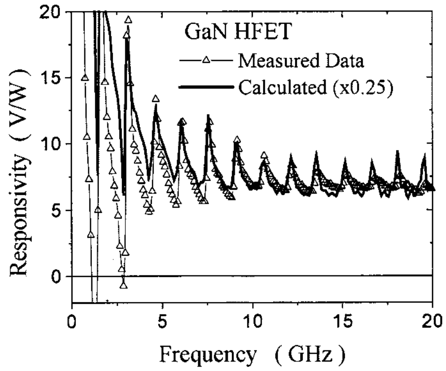

Fig. 5. Measured (symbols) and calculated (solid line) detector responsivity for a GaN HFET with the gate length $L = 5\ \mu$m, the gate bias $V_G = -1$ V, and the threshold voltage $V_T = -2$ V [7].

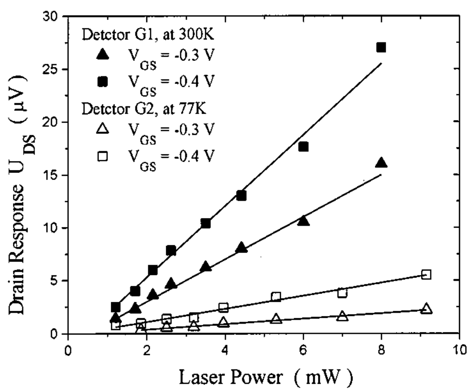

Fig. 6. AlGaAs/GaAs HEMT detector responses versus the intensity of the radiation for two detectors operating at 77 and 300 K. The linear relationship confirms that the HEMT operates as a square-law detector.

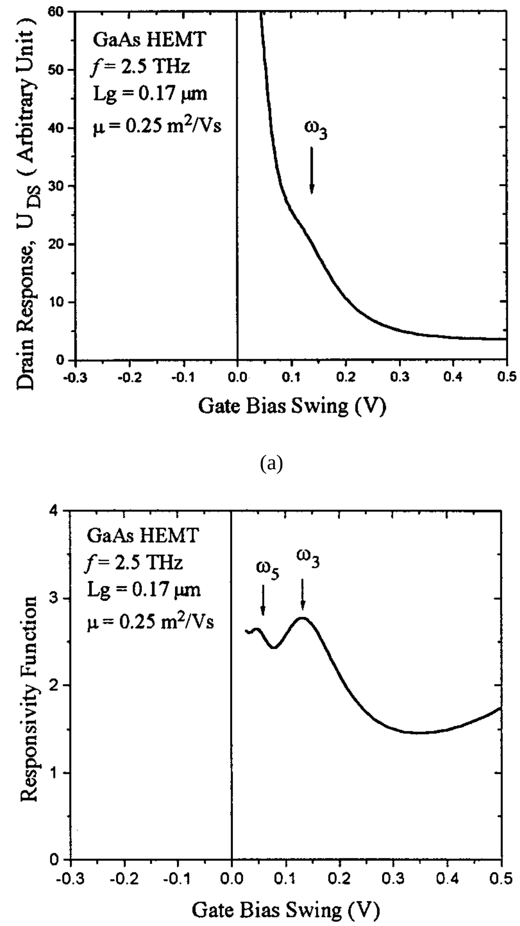

Fig. 7. Theoretical predictions of the responses for a GaAs HEMT-based detector with a mobility $\mu = 0.25$ m^2/V·s, and a gate length $L_g = 0.17\ \mu$m. The operating frequency is 2.5 THz. (a) Detector responses [dc drain voltage ($U_{\rm DS}$)] versus gate-bias swing ($V_{\rm GS} - V_T$). (b) Dimensionless responsivity function versus ($V_{\rm GS} - V_T$).

detectors [4], [6], [7], [13]. The dynamic range of such a detector is limited by the gate voltage swing because the responsivity decreases when the terahertz-radiation-induced ac voltage becomes on the order of a few percent of gate voltage swing [19].

Our recent experimental data (see [6]–[8], [20], and [21] and the results below) confirm many features of these theoretical predictions, but also pose many questions.

Fig. 5 shows measured and calculated frequency dependencies of the detector responsivity for a GaN heterostructure FET (HFET) with a cutoff frequency of approximately 2 GHz [7].

The periodic variation of the responsivity with frequency is caused by changes in the transmission-line impedance with frequency. As can be seen from Fig. 5, the device operates as broad-band nonresonant detector of microwave radiation at frequencies higher that the cutoff frequency and the measured data agree with the theory.

Fig. 6 shows the drain response $U_{\rm DS}$ of a 0.17-μm AlGaAs/GaAs HEMT detector to a 2.5-THz continuous wave (CW) laser [20].[1] The terahertz radiation, which was chopped and focused on the HEMT, induced a dc drain-to-source voltage $U_{\rm DS}$. $U_{\rm DS}$ was measured using a lock-in amplifier, which displayed the amplitude and the phase of $U_{\rm DS}$. Since the phase kept fairly constant during each measurement of this study, the value of $U_{\rm DS}$, in this paper, is just the amplitude read from lock-in display. Therefore, it is always positive. The detailed device fabrication and the measurement setup are described in [20] and [21]. As can be seen from Fig. 6, a fairly linear relationship between the drain response and laser power confirms that the HEMT operates as a square-law detector.

Fig. 7 shows the calculated drain voltage response versus gate-bias swing for a GaAs HEMT detector with a mobility of 0.25 m^2/V·s, an effective gate length of 0.17 μm, and zero electron fluid viscosity. The operating frequency is 2.5 THz. The fundamental resonant peak should occur at the gate-bias swing $U = V_{\rm GT} = (V_{\rm GS} - V_T) \approx 1$ V (not shown in Fig. 7). The third harmonic peak (denoted as ω_3) occurs at gate-bias swing $V_{\rm GT} = (V_{\rm GS} - V_T) \approx 0.13$ V. Here, $V_{\rm GS}$ is the gate-to-source bias and V_T is the HEMT threshold voltage. However, the gate leakage current limited the gate-bias swing to a value smaller than 0.8 V for an HEMT with a V_T close to -0.5 V. Therefore, the fundamental resonant peak could not be observed. The third harmonic resonant peak is very week and does not lead to a very

[1]Due to a calibration error, the scale in the original figures for 2.5 THz in [20] and [21] is incorrect. The measured drain voltage was, in fact, smaller by a factor of ten, as corrected in Figs. 6 and 8 in this paper.

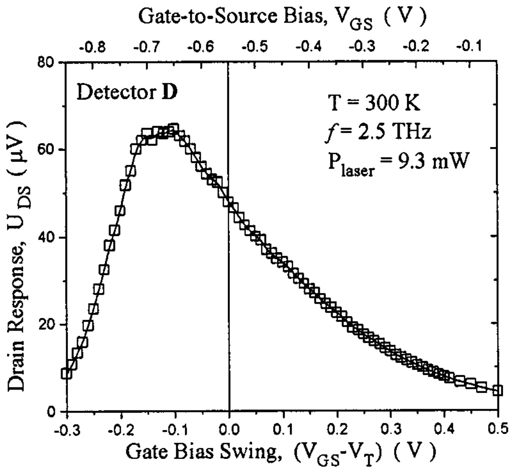

(a)

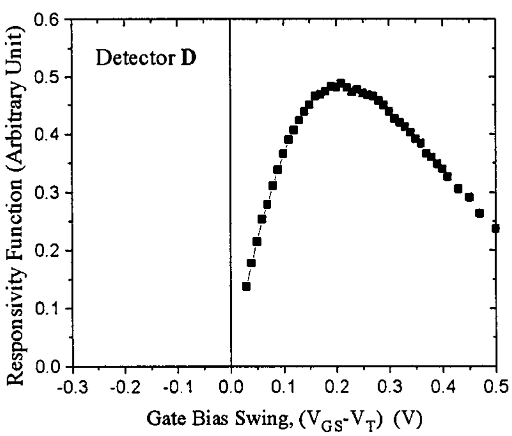

(b)

Fig. 8. Measured responses for AlGaAs/GaAs detector versus gate-bias swing ($V_{\rm GS} - V_T$). The extracted electron mobility, threshold voltage, and gate length from the device *I–V* characteristics are $\mu = 0.25$ m^2/V·s, $V_T = -0.55$ V, and $L_g = 0.17$ μm, respectively. The operating frequency is 2.5 THz. (a) Detector responses $U_{\rm DS}$. (b) Dimensionless responsivity function (defined as the product $U^*_{\rm DS}(V_{\rm GS} - V_T)$) [see (4)].

pronounced feature in the drain voltage response [see Fig. 7(a)]. As shown in [4], the measured response

$$U_{\rm DS} = |-\Delta U| = \frac{1}{4}\frac{U_a^2}{V_{\rm GT}} f(\omega) \quad (4)$$

where U_a is the amplitude of the ac source-to-gate voltage induced by the incoming radiation and $f(\omega)$ is a *dimensionless responsivity function*. The calculated responsivity function corresponding to the detector response shown in Fig. 7(a) is plotted in Fig. 7(b). As can be seen from the comparison of Fig. 7(a) and (b), the third harmonic peak is much more pronounced in the responsivity function. The drain voltage dependence on the gate bias is dominated in this case by the $1/V_{\rm GT}$ dependence [see (4)].

Therefore, we used the responsivity function (defined as the product $U^*_{\rm DS}V_{\rm GT}$) in order to identify the resonant detector response [21].

The experimental results confirmed that this terahertz detector response can be tuned by the gate bias (see Fig. 8).

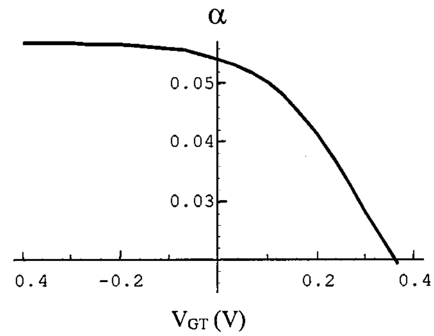

Fig. 9. DIBL constant as a function of the gate voltage swing using the default HEMT parameters in [22]. As can be seen, the detector response near threshold can drop because of the decreasing importance of the DIBL effect.

Above the threshold voltage ($V_T \sim -0.55$ V for Detector D in Fig. 8), the responsivity increases with the decreasing gate voltage as predicted by the detector theory [4]. This theory is only valid for $V_{\rm GS} > V_T$ and when the carrier density in the HEMT channel is high enough to form a 2-D electronic fluid. For $V_{\rm GS} \ll V_T$, the carrier density becomes too low, the parasitic leakage becomes dominant, the transistor stops operating as a transistor and, therefore, cannot respond to a terahertz signal. This is why the detector responsivity decreases to zero for $V_{\rm GS} < -0.65 < V_T$. However, in the subthreshold regime, the effect of the terahertz signal on the potential barrier separating the source and drain might become important. In this regime, the drain current $I_{\rm DS}$ at $V_{\rm DS} < kT/q$ is given by

$$I_{\rm DS} = g_0 V_{\rm DS} \exp\frac{V_{\rm GT} - \alpha V_{\rm DS}}{V_{\rm th}} \quad (5)$$

where α is the drain-induced barrier lowering (DIBL) constant, $V_{\rm th} = \eta kT$ is the effective thermal voltage, and η is the ideality factor. In HFET's, α is a function of the gate bias [22]. Fig. 9 shows a typical dependence of α on the $V_{\rm GT}$ (using default AIM-Spice parameters given in [22]). Assuming $V_{\rm DS} = U_{\rm DSo} + U_a \sin(\omega t)$ and equating the second-order Taylor expansion of the time-averaged drain current with respect to the drain voltage (to satisfy zero current for the open circuit at the drain), we obtain for the detector response

$$U_{\rm DSo} = -\alpha\, U_a^2/(2V_{\rm th}). \quad (6)$$

The measured detector response (using a lock-in amplifier) should be $U_{\rm DS} = |U_{\rm DSo}|$. This mechanism can possibly explain the detector response close to and below threshold.

Fig. 10 compares responsivity function [see (4)] measured at 77 and 300 K [21]. The threshold voltage of this HEMT is around −0.5 V at 300 K and −0.4 V at 77 K. The measured responsivity function exhibits a peak, which may correspond to the third harmonic (see below). However, we do not observe the expected large increase in responsivity function related to an increase in the mobility at cryogenic temperatures (see Fig. 10). The responsivity is possibly more strongly limited by the viscosity of the electronic fluid, which might have been underestimated in [3]. Also, the viscosity is more important at higher harmonics. Fig. 10 also shows the calculated responsivity (normalized to the measured data) for a detector with the mobilities of 0.25 m^2/V·s (for 300 K) and 0.8 m^2/V·s (for 77 K), the effective gate length of 0.17 μm, and for the viscosity values

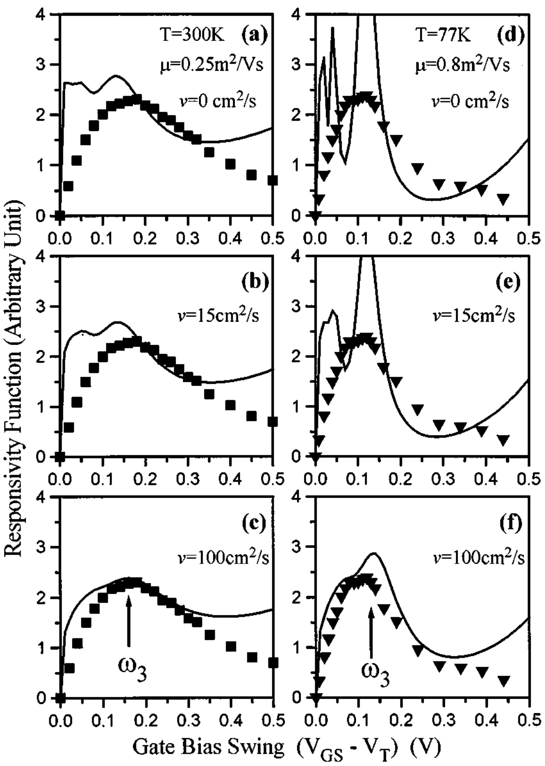

Fig. 10. Measured (symbols) and simulated (solid lines) gate-bias dependencies of responsivity function at 300 (left-hand side) and 77 K (right-hand side) and $f = 2.5$ THz for a AlGaAs/GaAs detector (Detector G). The parameters used for these calculations are $L_g = 0.17$ μm, $\mu = 0.25$ m^2/V·s for (a)–(c) and $\mu = 0.8$ m^2/V·s for (d)–(f), and three values of the viscosity of the electron fluid υ of 0, 15, and 100 cm^2/s. The peaks correspond to the third harmonic of the surface plasma frequency ω_3 [21].

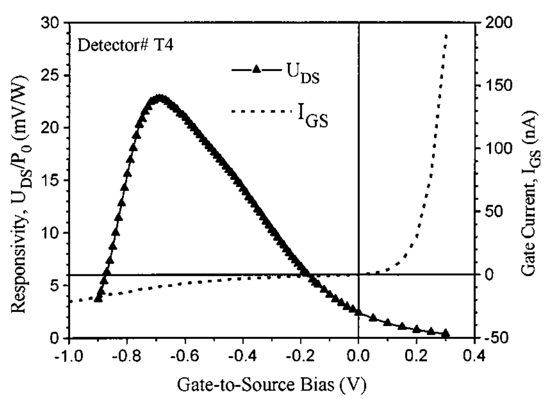

Fig. 11. Measured detector responsivity (symbols defined as $U_{\rm DS}/P_0$) at 2.5 THz and gate-to-source current (dashed line) versus gate-to-source bias for an AlGaAs/GaAs detector (Detector #T4).

of 0, 15, and 100 cm^2/s. These calculations show that, in principle, a higher viscosity can explain the observed temperature dependencies. As can be seen from Fig. 10, the position of the maximum of the responsivity function is very close to the third harmonic frequency ω_3, which is in agreement with the theory.

Fig. 11 compares the gate-bias dependencies of the detector responsivity and the gate-to-source currents. Since the drain current was zero (dc open circuit at the drain), and the gate current in the measurement range was very small (on the order of nanoampere), the heating effect should be entirely independent of the gate bias. Hence, it could not have been responsible for the measured gate-bias-dependent responsivity. Also, as shown in Fig. 11, the gate current decreases monotonously (from positive to negative) with decreasing gate bias, while the detector response reach a peak near the threshold ($V_T \approx -0.5$ V for this detector). Hence, the detector response could not be explained by the response of the Schottky gate.

We have also studied the detector response as a function of the angle between the ac electric field and the direction from the source to the drain (during these measurements, the electric field was always in the device plane). Our theory applies to the case when this angle is zero. However, the modulation of the electron sheet density by the terahertz radiation should also occur at other angles. We expected that the detector responsivity should decrease as a square of a cosine square function of the angle. The experimental data confirm a strong polarization dependence. However, the measured dependence is very sensitive to the sample position, which might affect the radiation coupling. Therefore, the polarization dependence might be complex, as was reported in [21]. It might be also affected by the excitation of the plasma waves with a wave vector component along the gate [12]. Such modes might be excited if the gate length varies slightly along the gatewidth due to technological nonuniformities.

IV. Conclusion

We reviewed theoretical predictions for plasma-wave generation and excitation in FET's and presented recent experimental data that show that an FET can operate as detection and generation of electromagnetic radiation in a broad range of frequencies from microwave to terahertz range, including frequencies far exceeding the transistor cutoff frequency.

Acknowledgment

The authors are grateful to Dr. J. Hesler and L. T. Suddarth, University of Virginia, Charlottesville, for their help with the measurements. The authors would also like to thank Dr. M. Dyakonov for useful discussions.

References

[1] M. I. Dyakonov and M. S. Shur, "Field effect transistor as two dimensional electronic flute," in *Proc. NATO Advanced Res. Workshop*, Ile de Bendor, France, July 1995, pp. 251–262.

[2] S. Luryi, J. Xu, and A. Zaslavsky, Eds., *Future Trends in Microelectronics. Reflection on the Road to Nanotechnology*. Norwell, MA: Kluwer, 1996, vol. 323.

[3] M. Dyakonov and M. S. Shur, "Shallow water analogy for a wallistic field effect transistor. New mechanism of plasma wave generation by DC current," *Phys. Rev. Lett.*, vol. 71, no. 15, pp. 2465–2468, 1993.

[4] ——, "Detection, mixing, and frequency multiplication of terahertz radiation by two dimensional electronic fluid," *IEEE Trans. Electron Devices*, vol. 43, pp. 380–387, Mar. 1996.

[5] M. V. Cheremisin, "Etude d'instabilites dans un liquide bidimensionnel d'electrons dans un transistor a effet de champ," Ph.D. dissertation, Dept. Phys., Univ. Montpellier, Montpellier, France, 1999.

[6] R. Weikle, J.-Q. Lü, M. S. Shur, and M. I. Dyakonov, "Detection of microwave radiation by electronic fluid in high electron mobility transistors," *Electron. Lett.*, vol. 32, no. 7, pp. 2148–2149, 1996.

[7] J.-Q. Lü, M. S. Shur, R. Weikle, and M. I. Dyakonov, "Detection of microwave radiation by electronic fluid in AlGaN/GaN high electron mobility transistors," in *Proc. 16th Biennial Conf. Advanced Concepts High-Speed Semiconduct. Devices Circuits*, Ithaca, NY, Aug. 1997, pp. 211–217.

[8] J.-Q. Lü, M. S. Shur, J. L. Hesler, L. Sun, and R. Weikle, "Terahertz detector utilizing two-dimensional electronic fluid," *IEEE Electron Device Lett.*, vol. 19, pp. 373–375, Oct. 1998.

[9] M. I. Dyakonov and M. S. Shur, "Two dimensional electronic flute," *Appl. Phys. Lett.*, vol. 67, no. 8, pp. 1137–1139, 1995.

[10] F. J. Crowne, "Contact boundary conditions and the Dyakonov-Shur instability in high electron mobility transistors," *J. Appl. Phys.*, vol. 82, no. 3, pp. 1242–1254, Aug. 1997.

[11] S. Rudin and G. Samsonidze, "Edge and strip plasmons in a two-dimensional electron fluid," *Phys. Rev. B, Condens. Matter*, vol. 58, no. 24, pp. 16369–16373, Dec. 1998.

[12] I. Gornyi, private communication, 1997.

[13] M. I. Dyakonov and M. S. Shur, "Plasma wave electronics: Novel terahertz devices using two dimensional electron fluid," *IEEE Trans. Electron Devices*, vol. 43, pp. 1640–1646, Oct. 1996.

[14] M. Dyakonov, private communication, 1999.

[15] A. V. Chaplik, "Possible crystallization of charge carriers in low-density inversion layers," *Zh. Eksp. Teor. Fiz.*, vol. 62, pp. 746–753, 1972.

[16] M. Nakayama, "Theory of surface waves coupled to surface carriers," *J. Phys. Soc.*, vol. 36, pp. 393–398, 1974.

[17] M. V. Cheremisin, M. I. Dyakonov, M. S. Shur, and G. Samsonidze, "Influence of electron scattering on current instability in field effect transistor," *Solid State Electron.*, vol. 42, no. 9, pp. 1737–1742, 1998.

[18] M. Dyakonov and M. S. Shur, "Choking of electron flow—A mechanism of current saturation in field effect transistors," *Phys. Rev. B, Condens. Matter*, vol. 51, no. 20, pp. 14341–14345, 1995.

[19] G. Samsonidze, S. Rudin, and M. S. Shur, "Large signal theory of plasma electronics terahertz detector," in *IEEE Proc. 6th Int. Conf. Terahertz Electron.*, Leeds, U.K., 1998, pp. 231–233.

[20] M. S. Shur, J.-Q. Lü, and M. Dyakonov, "Plasma wave electronics: Terahertz sources and detectors using two dimensional electronic fluid in high electron mobility transistors," in *IEEE Proc. 6th Int. Conf. Terahertz Electron.*, Leeds, U.K., 1998, pp. 127–130.

[21] J.-Q. Lü, M. S. Shur, J. L. Hesler, L. Sun, and R. Weikle II, "A resonant terahertz detector utilizing a high electron mobility transistor," in *IEDM Tech. l Dig.*, San Francisco, CA, 1998, pp. 453–456.

[22] T. Fjeldly, T. Ytterdal, and M. S. Shur, *Introduction to Device and Circuit Modeling for VLSI*. New York: Wiley, 1998.

Michael S. Shur (M'79–SM'83–F'89) received the M.S.E.E. degree (with honors) from St. Petersburg Electrotechnical Institute, St. Petersburg, Russia, in 1965, the Ph.D. degree in physics and Doctor of Physics and Mathematics from A. F. Ioffe Institute of Physics and Technology, St. Petersburg, Russia, in 1967 and 1992, respectively.

He is the Patricia W. and C. Sheldon Roberts'48 Professor of Solid State Electronics and Associate Director of the Center for Integrated Electronics and Electronics Manufacturing, Rensselaer Polytechnic Institute, Troy, NY. He is the Editor-in-Chief of the *International Journal of High Speed Electronics and Systems*.

Dr. Shur is a Fellow of the American Physical Society, and a member of Eta Kappa Nu and Tau Beta Pi. From 1990 to 1993, he served as an associate editor of the IEEE TRANSACTIONS ON ELECTRON DEVICES. In 1994, he was awarded an Honorary Doctorate by the Saint Petersburg State Technical University. He also co-authored a paper that received the Best Paper Award at 1998 Government Microcircuits Applications Conference (GOMAC'98).

Jian-Qiang (James) Lü (M'97) received the B.S. degree from the Shanxi Normal University, Linfen, China, in 1983, the M.S. degree from the Peking Normal University, Peking, China, in 1986, and the Dr. rer. nat. (Ph.D.) degree from the Technical University of Munich, Munich, Germany, in 1995.

He has held research or faculty positions at the Peking Normal University, Beijing University of Posts and Telecommunications, Technical University of Munich, and the University of Virginia (UVA). In 1997, he joined Rensselaer Polytechnic Institute (RPI), Troy, NY, as a Research Scientist, and was appointed a Research Assistant Professor in 1999. He has been involved in the field of high Tc superconductor, ion implantation and ion beam mixing, silicon device reliability and device related defects, and optoelectronics. His current research interests include the design, fabrication, and testing of novel electron devices, interconnects, and advanced packaging, such as plasma-wave electronics devices for terahertz applications, heterodimensional FET devices for low-power applications, novel devices using Si–Ge quantum dots and dots array, GaN high-power devices, and three-dimensional (3-D) integrated-circuit (IC) chip stacking. He and his colleagues fabricated and tested the first plasma-wave detectors operating at gigahertz frequency (in 1996 at UVA), and at terahertz frequency (in 1998 at RPI).

Dr. Lü is a member of the Amercian Physical Society. He was a Deutsche Akademischer Austauschdienst Scholar (1990–1992) and the recipient of a Best Paper Award presented at the Third Annual Academic Conference of Manufacturing Technology, Chinese Electronics Society, Chengdu, China, 1987.